(12)

Hydrogen Embrittlement in 17-4PH Stainless Steel

by
Kenneth R. Hayes
Engineering Department

AUGUST 1982
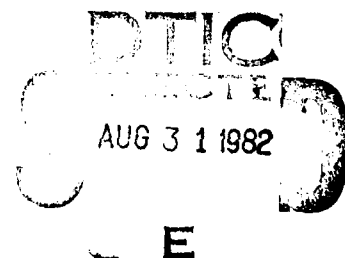
**NAVAL WEAPONS CENTER
CHINA LAKE, CALIFORNIA 93555**

DTIC

AUG 3 1 1982

E

Naval Weapons Center
AN ACTIVITY OF THE NAVAL MATERIAL COMMAND

FOREWORD

A study investigating the influence of internal hydrogen on mechanical properties of 17-4PH stainless steel was authorized by the Naval Air Systems Command under Task Assignment A542204i/0086/1000/000001. The experimental work was performed during the summer of 1981. The purpose of this study was to (1) investigate the mechanism of hydrogen embrittlement of precipitation hardening steels, and (2) optimize the metallurgical structure (heat treatment) of 17-4PH stainless steel to develop resistance to hydrogen embrittlement, consistent with strength requirements. This report is the first of a series investigating factors influencing environmental degradation of structural materials used in missile applications.

This report was reviewed for technical accuracy by Dr. G. T. Murray and Dr. G. A. Hayes.

Approved by
D. J. RUSSELL, *Head*
Engineering Department
23 June 1982

Under authority of
J. J. LAHR
Capt., U.S. Navy
Commander

Released for publication by
B. W. HAYS
Technical Director

NWC Technical Publication 6343

REPORT DOCUMENTATION PAGE		READ INSTRUCTIONS BEFORE COMPLETING FORM
1. REPORT NUMBER NWC TP 6343	2. GOVT ACCESSION NO. AD- A118716	3. RECIPIENT'S CATALOG NUMBER
4. TITLE (and Subtitle) HYDROGEN EMBRITTLEMENT IN 17-4PH STAINLESS STEEL		5. TYPE OF REPORT & PERIOD COVERED Final Report 1981 – 1982
		6. PERFORMING ORG. REPORT NUMBER
7. AUTHOR(s) Kenneth R. Hayes		8. CONTRACT OR GRANT NUMBER(s)
9. PERFORMING ORGANIZATION NAME AND ADDRESS Naval Weapons Center China Lake, CA 93555		10. PROGRAM ELEMENT, PROJECT, TASK AREA & WORK UNIT NUMBERS Task Assignment A5422041/ 0086/1000/000C01
11. CONTROLLING OFFICE NAME AND ADDRESS Naval Weapons Center China Lake, CA 93555		12. REPORT DATE August 1982
		13. NUMBER OF PAGES 26
14. MONITORING AGENCY NAME & ADDRESS(if different from Controlling Office)		15. SECURITY CLASS. (of this report) UNCLASSIFIED
		15a. DECLASSIFICATION/DOWNGRADING SCHEDULE

16. DISTRIBUTION STATEMENT (of this Report)

Approved for public release; distribution unlimited.

17. DISTRIBUTION STATEMENT (of the abstract entered in Block 20, if different from Report)

18. SUPPLEMENTARY NOTES

19. KEY WORDS (Continue on reverse side if necessary and identify by block number)

Hydrogen Embrittlement   Strain Rate
17-4PH Stainless Steel   Fractography
Mechanical Properties

20. ABSTRACT (Continue on reverse side if necessary and identify by block number)

See back of form.

(U) *Hydrogen Embrittlement in 17-4PH Stainless Steel*, by Kenneth R. Hayes. China Lake, Calif., Naval Weapons Center, August 1982, 26 pp. (NWC TP 6343, publication UNCLASSIFIED.)

(U) Tensile and Charpy impact test specimens of 17-4PH stainless steel in Conditions A, H900, H950, H1000, H1050, H1100, H1150 and H1150M were cathodically charged with hydrogen for various lengths of time. After charging, the specimens were mechanically tested at room temperature. The tensile tests were conducted at strain rates of 0.02, 0.2, 2.0, and 20 min^{-1}.

(U) Changes in mechanical properties (reduction in area, ultimate strength, hardness) were correlated with heat treatment, hydrogen charging level, and strain rate. Scanning electron microscope (SEM) fractography was employed to characterize fracture surfaces and provide information concerning the failure modes that were operating.

(U) In the tensile investigation, hydrogen charging was shown to greatly reduce the percent reduction in area (% RA) of 17-4PH stainless steel in all heat treatment conditions. The decreases became more pronounced as the yield and ultimate strengths increased and with increased charging time. For a given charging treatment and aging condition the % RA was shown to be a function of strain rate, the largest decrease in % RA being measured at intermediate strain rates.

CONTENTS
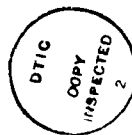
ACKNOWLEDGMENT

DTIC COPY INSPECTED 2

Accession For

NTIS GRA&I	X
DTIC TAB	☐
Unannounced	☐
Justification	

By
Distribution

Availability Codes

Avail and/or

Dist Special

A

1

INTRODUCTION

Due to their attractive mechanical properties, the precipitation hardenable (PH) martensitic stainless steels are used for many applications, particularly in the aerospace industry. These alloys possess aged yield strengths in the 965 MPa (140 KSI) to 1379 MPa (200 KSI) range, good toughness and corrosion resistance. However, in the past 20 years, evidence has been presented which indicates that there is considerable susceptibility to stress corrosion cracking (SCC) and hydrogen embrittlement (HE) in components produced from these steels. One early example of this was the failure of 17-4PH* stainless steel valve bolts on Titan III missiles (Reference 1). More recently, cadmium plated coupling rings and bolts manufactured from 17-4PH stainless steel used on Navy Sidewinder missiles have experienced HE (Reference 2).

It is generally recognized (References 3, 4, 5, 6) that the susceptibility of PH steels to HE can be minimized through proper control of heat treatment. Fujii (Reference 7) reported that 17-4PH stainless steel was sensitive to SCC at high strength levels but relatively insensitive in the overaged condition. The effect of an applied cathodic potential suggested the involvement of hydrogen. Fracture toughness measurements of 17-4PH stainless steel by Capeletti (Reference 8) were greatly reduced when tested under high hydrogen gas pressures. A minimum toughness was obtained with peak-aged specimens tested at high hydrogen pressures. Also noted was the change in fracture mechanism, from predominately ductile rupture in helium to cleavage in high-pressure hydrogen. At low hydrogen pressures, the fracture was determined to be mixed mode (quasi-cleavage and dimpled rupture).

There appears to be disagreement as to the degree that microstructure and or strength affects hydrogen induced ductility loss in steel. Because of this apparent disagreement and because of a lack of engineering data, work was initiated to characterize the effect of hydrogen on PH stainless steels.

This report presents the results of a detailed study investigating the influence of aging temperature, hydrogen charging level, and strain rate on the susceptibility of 17-4PH stainless steel heat-treated to a wide range of strength levels.

---

* ARMCO steel, registered trademark

EXPERIMENTAL PROCEDURE

Rods of 17-4PH stainless steel 2.54cm (1 in) in diameter were obtained from a single heat in the solution treated condition (Condition A) from ARMCO Steel Corporation. The composition of the material was determined to be: 0.041 C, 0.72 Mn, 0.33 Si, 3.44 Cu, 16.45 Cr, 4.67 Ni, 0.43 Cb, balance Fe. Smooth sub-size tensile specimens 0.508cm (0.200 in) thick conforming to ASTM specification E8 were machined from the rods.

Several different aging treatments were utilized to produce a wide range of microstructures and strength levels in the tensile specimens. A series of specimens was aged to each of the following conditions: H900, H950, H1000, H1050, H1150, and H1150M. These heat treatments produced a wide range of mechanical properties typically required for engineering applications of 17-4PH stainless steel. All specimens except the H900 and H1150M received a 4-hour aging treatment. The H900 tensile bars were aged for 1 hour at 482°C (900°F) while the H1150M specimens were double overaged by heat treating at 760°C (1400°F) for 2 hours, air cooling, then aging at 621°C (1150°F) for 4 hours. All specimens were air-cooled after aging. Figure 1 illustrates the wide range in microstructure brought about by the varying heat treatments. Specimens that were given these aging treatments, along with specimens in Condition A, were the control group for this investigation.

Hydrogen was introduced into the tensile specimens by means of cathodic charging. The specimens were immersed at room temperature in a 10% H_2SO_4 solution containing 10mg/liter of As_2O_3 being used as a poison to promote absorption of atomic hydrogen.[3] A current density of 9ma/cm^2 was employed for times varying from 0.5 to 24 hours.

Tensile and hardness tests were conducted immediately after charging (except for recovery tests) in air at room temperature. An Instron test machine was utilized to produce strain rates varying from 0.005 to 50.8cm/min (0.002 to 20 in/min). The specimens were tested to failure, all fracturing within the gage length. Percent reduction in area (% RA) at fracture was chosen as a measure of the degree of HE incurred by the test specimens. Percent RA was measured by micrometer.

A limited study concerning the influence of hydrogen on impact properties of 17-4PH stainless steel was also conducted in the course of this investigation. Charpy impact specimens were machined to ASTM specification E23. Aging treatments for the charpy specimens and tensile specimens were concurrent, and the charging procedures were identical for both sets of specimens. Room temperature impact testing was performed immediately after charging.
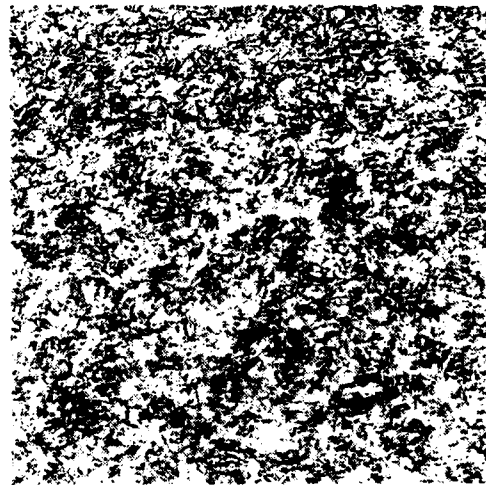
SEM fractography and optical microscopy were employed to characterize fracture surfaces and provide information concerning the failure modes that were operating.
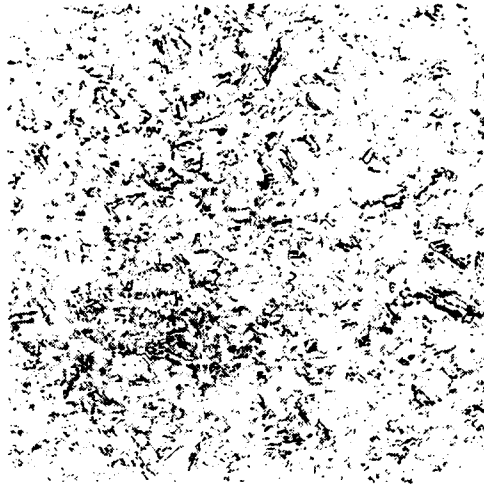
(a)

(b)

(c)

FIGURE 1. The Microstructure of 17-4PH Stainless Steel
Heat-Treated to Conditions (a) H1000, (b) H1050, and
(c) H1150. Etchout: Villela's Etch. 220X

RESULTS

The result of hydrogen charging 17-4PH stainless steel was examined from its effect on mechanical properties and fracture mode. A summary of mechanical property data of charged 17-4PH steel as a function of heat treatment and strain rate is presented in Table 1.

HARDNESS

The hardness data (Figure 2) showed that hydrogen charged specimens exhibited a consistent increase in hardness of from one to three Rockwell C points when compared to the values for uncharged specimens. Although the effect was small, it appears real in that it was observed for all aging conditions. Each data point represents an average of at least three independent hardness measurements.

CHARPY ENERGY

Charpy impact tests were performed and it was found that in general, hydrogen charged specimens had comparable impact properties to uncharged specimens. The one exception was that in the solution treated condition which showed a significant loss of impact energy when charged. This is not surprising since it is generally agreed that untempered martensite is the most susceptible microstructure to HE (Reference 9). Figure 3 is a plot of charpy energy versus ultimate tensile strength of 17-4PH, and shows the decrease in impact energy associated with the strength increase, as well as the charged versus uncharged impact energy results.

TENSILE

It was observed that ductility as measured by % RA was affected in all aging treatments of the 17-4PH stainless steel when charged with hydrogen. Figure 4 illustrates that the heat-treated condition of the specimen had some influence on the degree to which specimens were embrittled. For example, the H900 specimen decreased in ductility from 57.9% RA to 0.4% RA upon charging while the double overaged H1150M tensile bar only decreased from 68.4% RA to 40% RA.

The effect of hydrogen charging time on HE was studied by varying this time from 0.5 hour to 24 hours. The results of the four aging treatments investigated are plotted in Figure 5 as % RA versus charging time. It is apparent that higher aging temperatures lead to less severe HE. In 0.5 hour of charging, the H900 and H1000 specimens lost approximately 50% of their ductility. The lower strength H1150 and H1150M specimens required approximately 16 hours of charging to incur an equivalent loss.

A series of recovery tests was performed to evaluate the reversibility of HE for the charged 17-4PH stainless steel tensile bars.

TABLE 1. Mechanical Properties of Hydrogen Charged 17-4PH Stainless Steel.

| Condition		Strain Rate (min^{-1})	Hardness (Rc)	UTS (MPa)	RA (%)
A					
	NC*	0.2	35.5	1021	65.8
	NC	2.0	45.1	1436	52.2
16 hr	C	0.2	37.3	1089	4.7
H900					
	NC	0.2	44.9	1412	57.9
0.5 hr	C	0.2	45.1	1385	25.7
2.0 hr	C	0.2	46.3	1254	6.3
4.0 hr	C	0.2	45.8	1121	1.8
16 hr	C	0.2	46.1	597	0.4
16 hr	C	0.02	46.2	208	0
16 hr	C	2.0	47.0	1001	0
16 hr	C	0.002	46.3	115	0
H950					
	NC	0.2	39.1	1194	61.0
16 hr	C	0.2	41.6	1005	1.9
H1000					
	NC	0.2	38.7	1137	61.2
0.5 hr	C	0.2	38.9	1124	33.7
2.0 hr	C	0.2	39.8	1097	8.6
4.0 hr	C	0.2	38.0	1099	1.6
16 hr	C	0.2	39.1	780	0.4
16 hr	C	0.002	39.8	918	3.5
16 hr	C	0.02	40.1	785	1.9
16 hr	C	2.0	41.4	1039	0.4
16 hr	C	20.0	38.9	1162	14.4
H1000					
16 hr	C plus 16 hr Age	0.2	38.1	1124	9.6
16 hr	C plus 40 hr Age	0.2	37.7	1101	29.4
16 hr	C plus 0.4 hr Bake @204°C	0.2	37.7	1100	63.4
H1050					
	NC	0.2	36.0	1070	61.9
16 hr	C	0.2	37.5	1040	0.2
H1150					
	NC	0.2	32.0	963	64.9
0.5 hr	C	0.2	32.2	930	59.3
2.0 hr	C	0.2	32.6	934	49.1
16 hr	C	0.2	33.4	911	13.7
24 hr	C	0.2	33.4	937	21.7
16 hr	C	0.02	32.7	900	16.4
16 hr	C	2.0	33.4	980	14.9
16 hr	C	20.0	34.3	993	27.0
H1150M					
	NC	0.2	28.6	904	68.4
	NC	2.0	29.0	901	64.2
0.5 hr	C	0.2	28.9	918	63.2
2.0 hr	C	0.2	29.0	906	52.8
16 hr	C	0.2	28.6	822	40.0
24 hr	C	0.2	29.1	865	27.6
16 hr	C	0.02	29.2	872	44.8
16 hr	C	2.0	29.1	885	31.5
16 hr	C	20.0	30.3	913	44.7

* NC: No charge
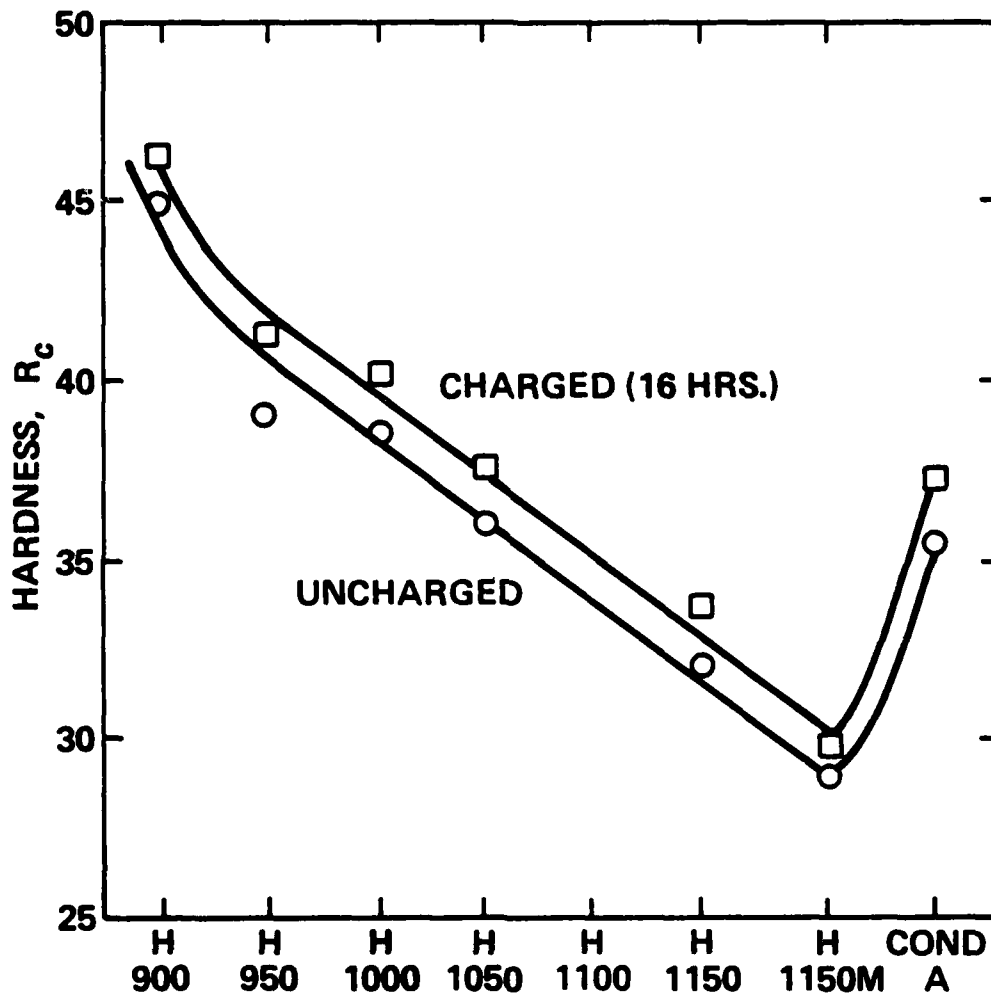
FIGURE 2. The Influence of Hydrogen Charging on the Hardness of 17-4PH in Various Aged Conditions.
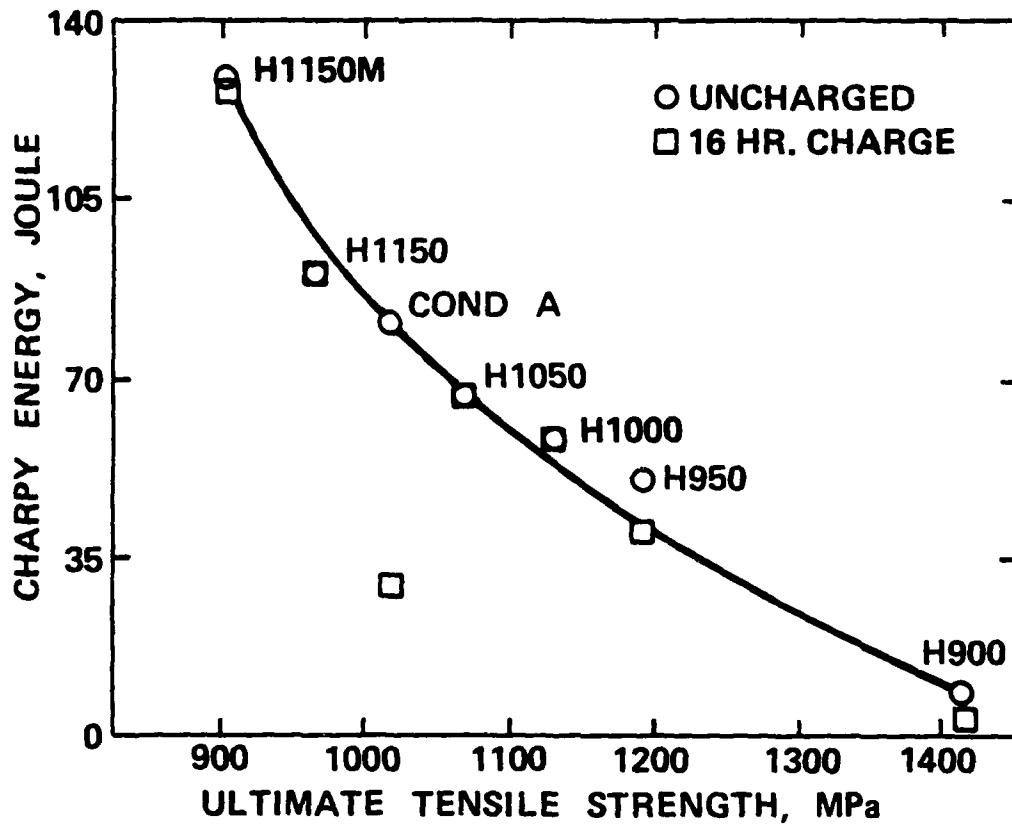
FIGURE 3. Charpy Impact Energy of Hydrogen Charged and Uncharged Specimens of Varying Ultimate Tensile Strength.
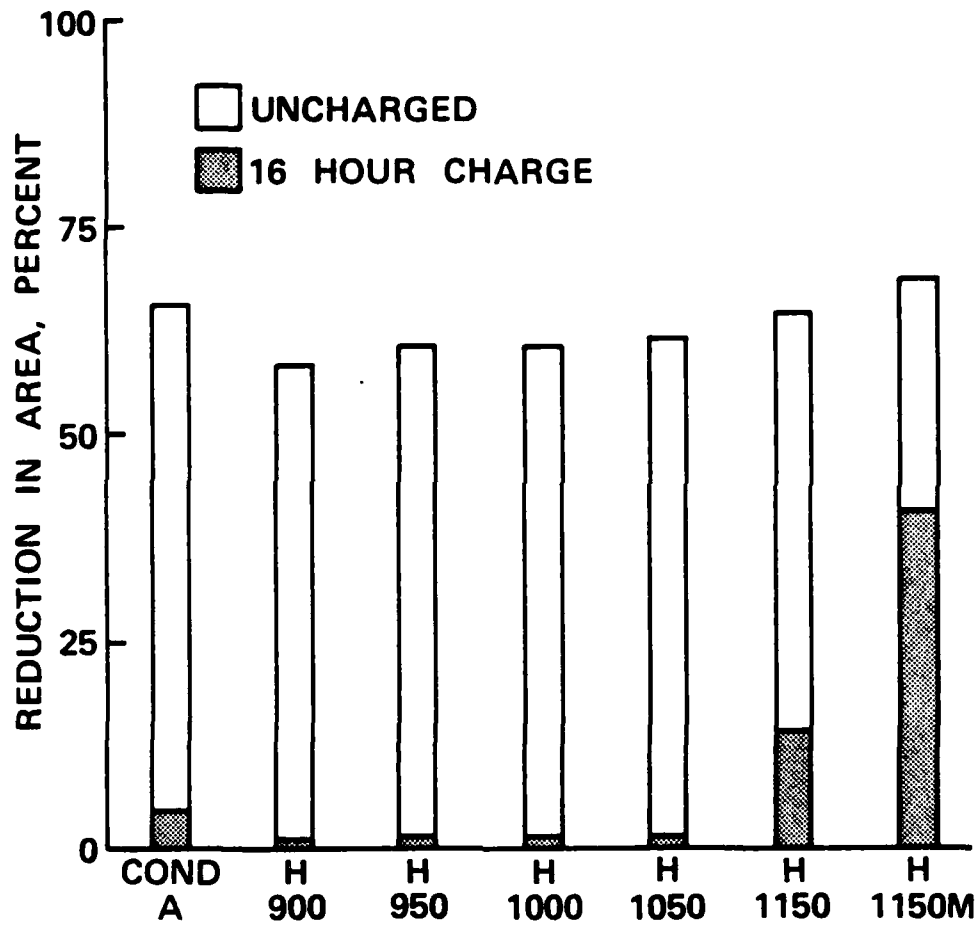
9

FIGURE 4. Influence of Hydrogen Charging
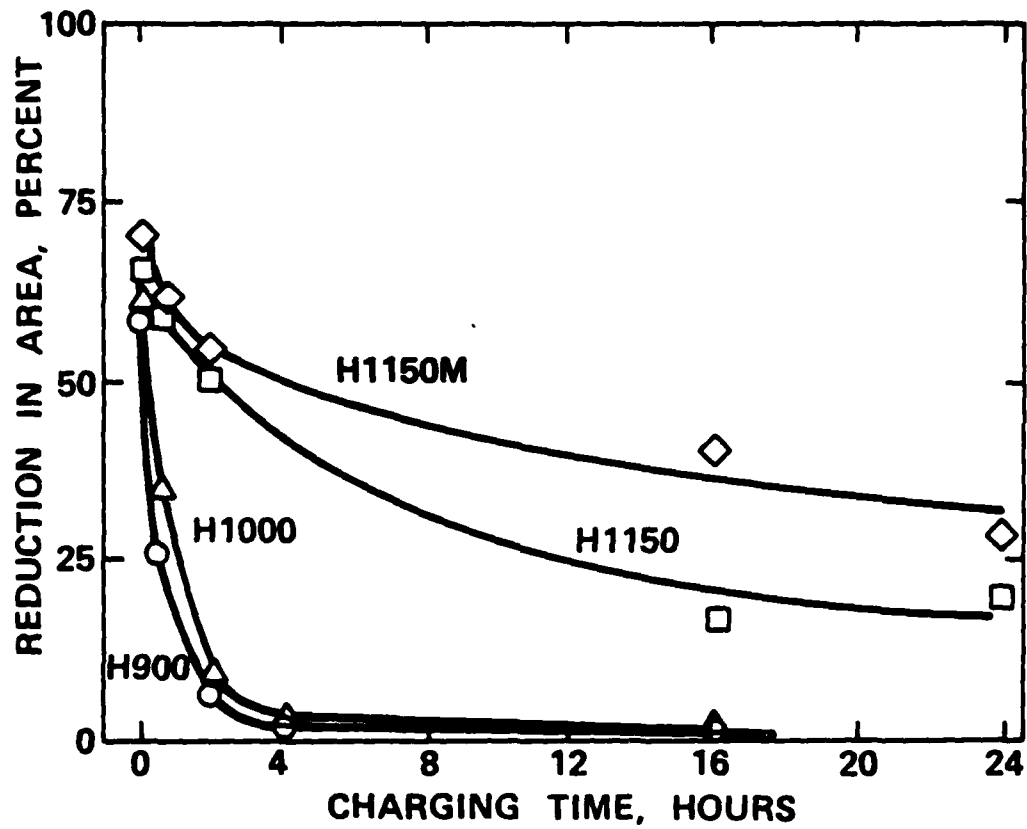% RA of 17-4PH in Various Aged Conditions.

FIGURE 5. The Effect of Hydrogen Charging
Time on % RA of Heat-Treated 17-4PH.

11

Three specimens in condition H1000 were charged for 16 hours. Two of the specimens were allowed to stand at room temperature for 16 hours and 40 hours respectively. The third specimen was baked at 204°C for 4 hours. At the end of the recovery treatment, tensile test data indicated that significant ductility was recovered, going from 0.4% RA for a 16-hour charge with no recovery to 29.4% RA for a 16-hour charge followed by a 40-hour recovery. The baked specimen completely regained its ductility, showing 63.4% RA compared to 61.2% RA for an uncharged specimen (Figure 6).

The effect that charging time had on the ultimate tensile strength (UTS) can be seen in Figure 7. It is apparent that the high strength H900 condition lost considerable UTS with increasing charging time while the more ductile, low strength H1150 condition was not significantly affected. This is consistent with the results of other investigations (References 10, 11) which explain that hydrogen decreases ductility, leading to less workhardening, thus decreasing the UTS. However, in the case of 17-4PH very little workhardening occurs. Consequently the reason for the decrease in UTS of high strength 17-4PH after hydrogen charging may be related to relative resistance to crack propagation. In the high strength, low fracture toughness condition, hydrogen assisted crack propagation is not readily arrested and failure occurs at lower UTS than in the uncharged condition. In the lower strength conditions, hydrogen assisted crack propagation is more readily arrested by the tougher material, and UTS is affected to a lesser degree.

The final variable investigated in this study was that of strain rate. As described earlier, a series of tensile specimens that were charged 16 hours were tested with strain rates varying from 0.002 min^{-1} to 20.0 min^{-1}. This was performed for each of the following heat treatments: H900, H1000, H1150, and H1150M. Percent RA plotted versus strain rate for the four treatments is presented in Figure 8. While the H900 condition seemed unaffected by loading rate, the other three treatments showed varying degrees of sensitivity to the strain rate. All three exhibited minimum values of % RA for strain rates in the vicinity of 0.2 min^{-1} to 2.0 min^{-1}. At the same time, some loss of % RA was observed no matter what strain rate was employed. Typical of the three treatments was that for condition H1150. At a strain rate of 0.02 min^{-1} the RA was measured to be 16.4%. This decreased to a minimum value of 13.7% RA at 0.2 min^{-1}. At a strain rate of 20 min^{-1} the RA increased to 27.0%.

MACROEXAMINATION

In most cases, visual examination of the fracture surfaces showed a distinct shell near the exterior of the hydrogen charged specimens. Figure 9 is a series of fractographs of specimens aged to condition H1000 and hydrogen charged for varying times. It can be seen that as the charging time increases, the shell thickness also increases. The thickness of the shell plotted against the hydrogen charging time is shown in Figure 10.
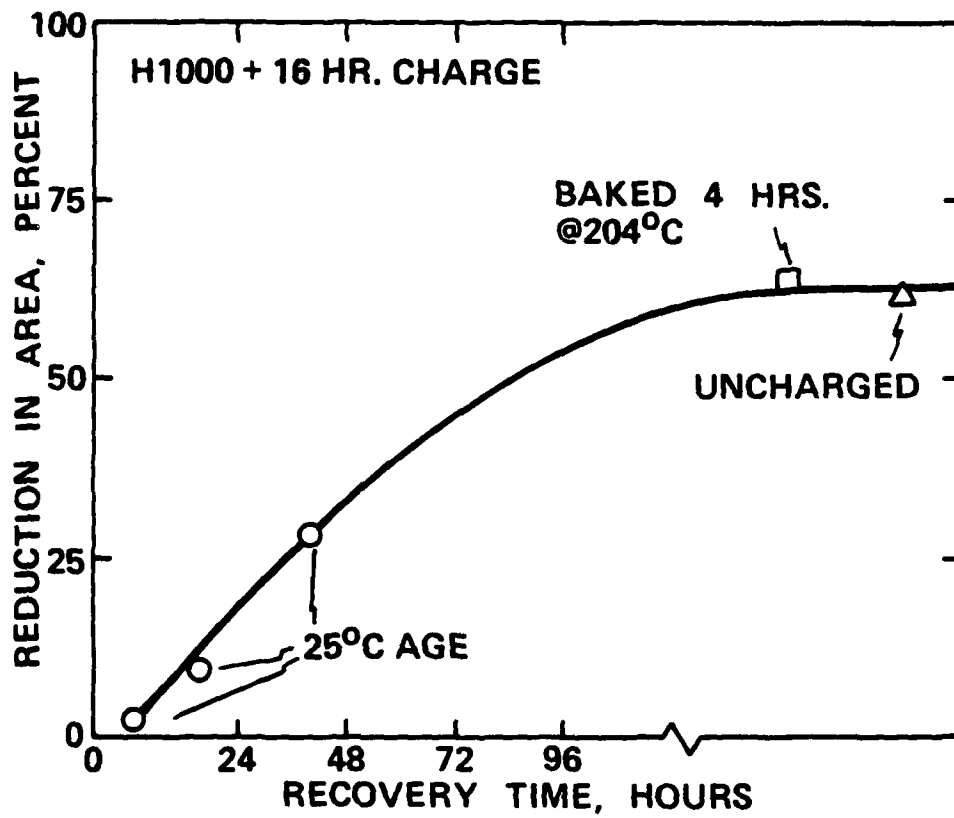
12

FIGURE 6.   Recovery of % RA in Hydrogen
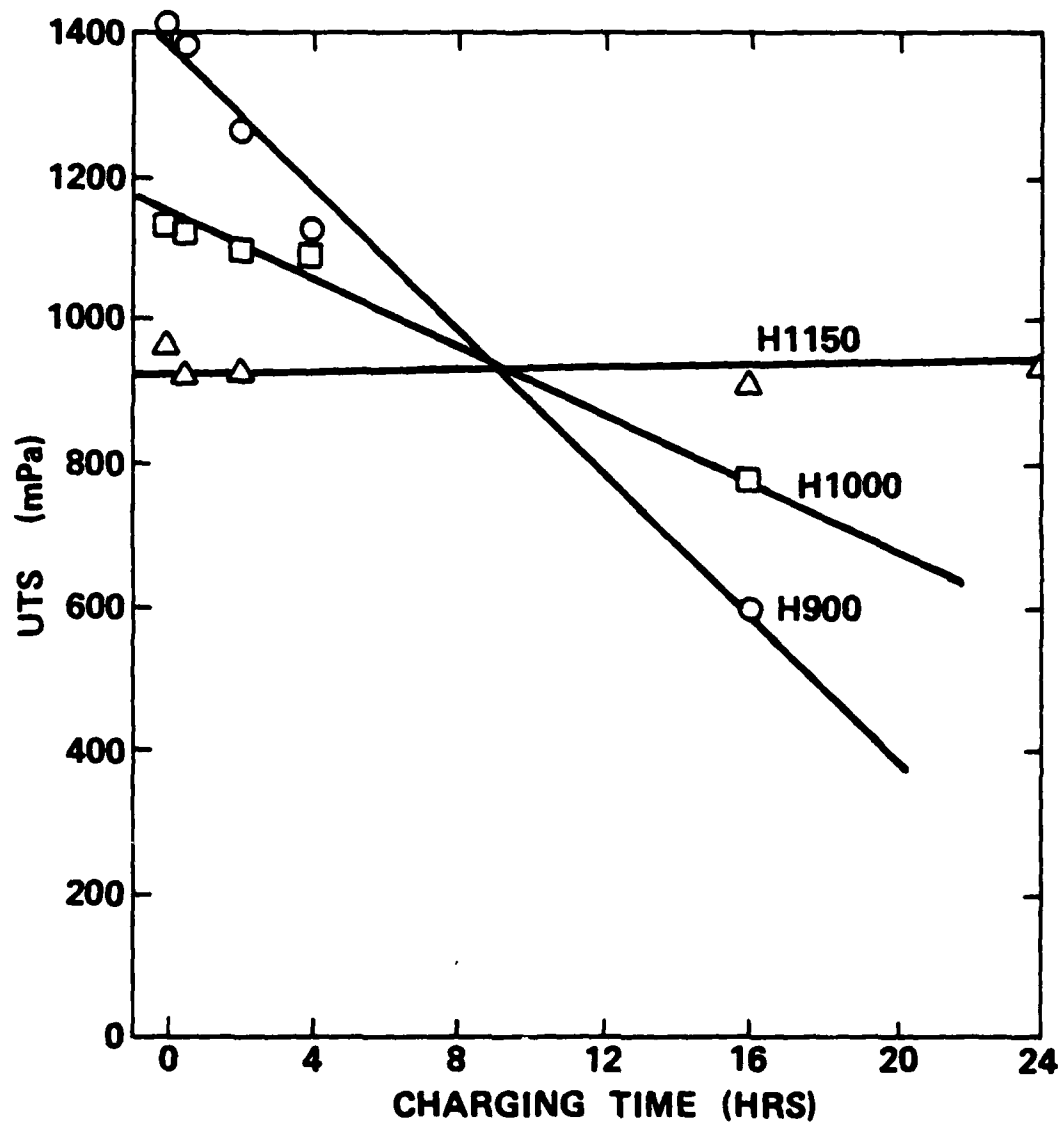Charged 17-4PH in Condition H1000.

FIGURE 7. Variation in Ultimate Tensile Strength with
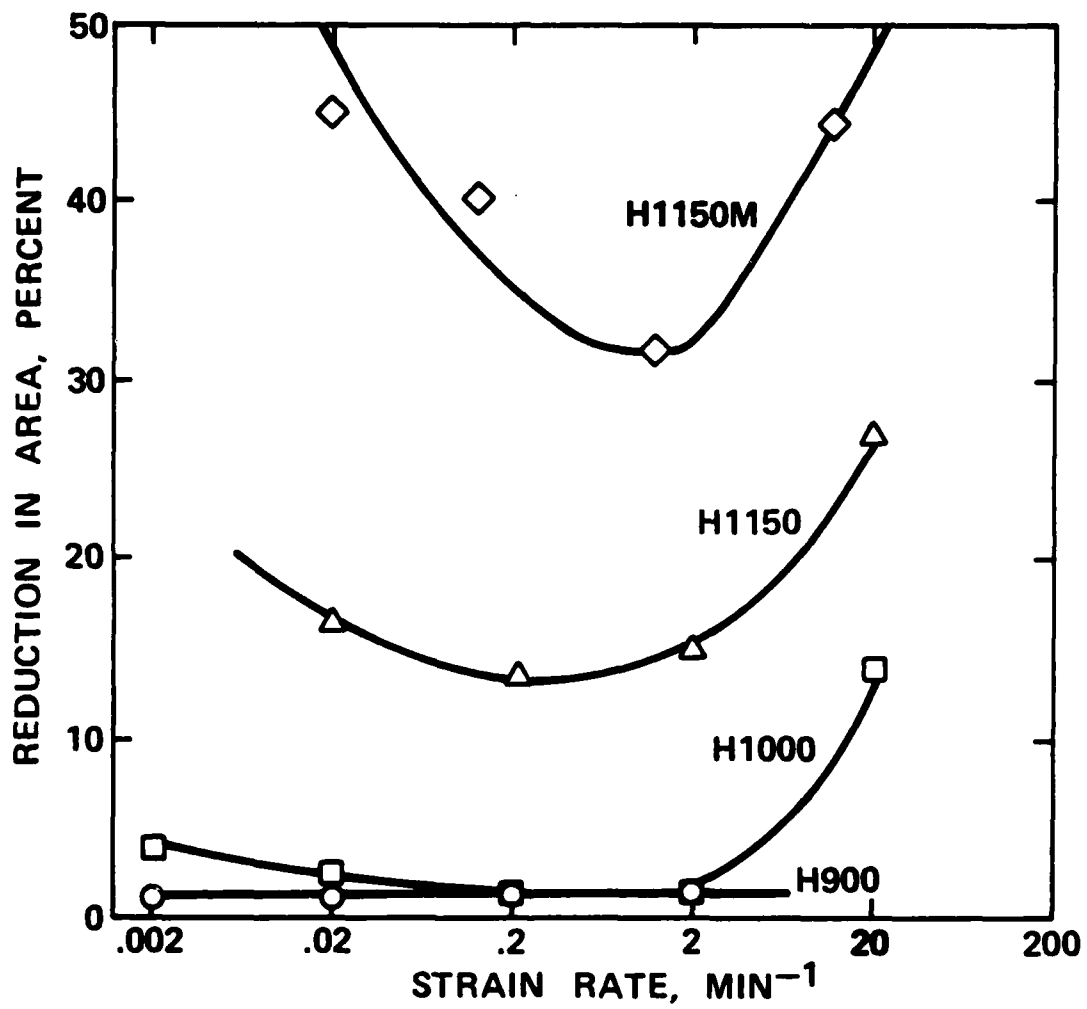Hydrogen Charging Time for 17-4PH in Various Aged Conditions.

14

FIGURE 8.   The Influence of Strain Rate on % RA of
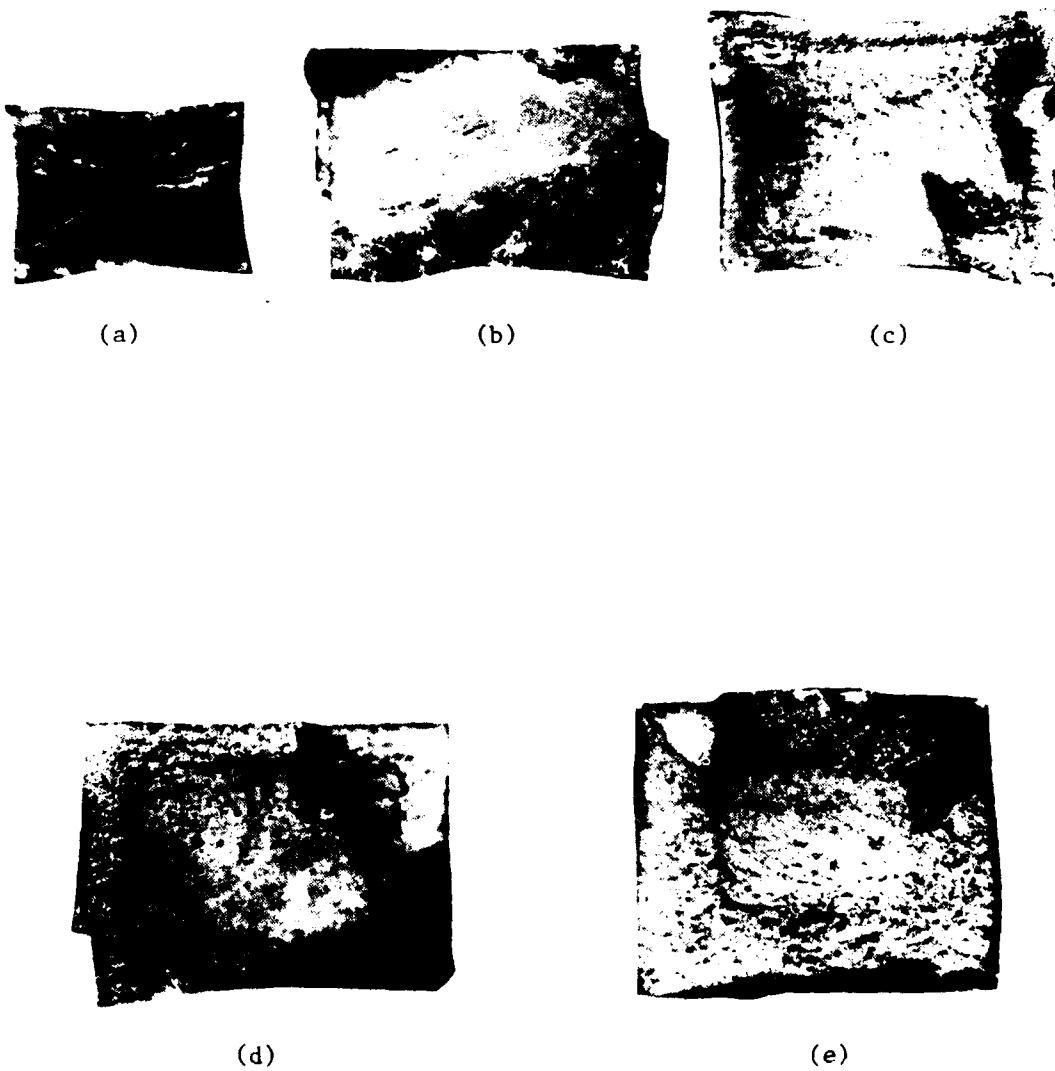Hydrogen Charged 17-4PH in Various Aged Conditions.

(a)   (b)   (c)

(d)   (e)

FIGURE 9. Fracture Surfaces of 17-4PH Tensile Specimens Aged
to Condition H1000, Then Hydrogen Charged for (a) 0 hour,
(b) 0.5 hour,   (c) 2.0 hours, (d) 4.0 hours, and (e) 16 hours.

16

It should be noted that the aging treatment had a pronounced effect on the shell thickness. This shell was later determined to be a zone of transgranular and intergranular fracture, while the interior structure was that of dimpled rupture. In the case of both the H900 and H1000 conditions, the shell thickness increased with charging time until it extended across the complete cross section of the tensile bars.

MICROSCOPY

SEM fractography was employed to characterize the fracture behavior of the embrittled material. The specimens observed were in the H900, H1000, H1150, and H1150M conditions with a common charging time of 2 hours. In each specimen (Figures 11-14) it can be observed that the structure ranges from dimpled rupture in the center to a type of brittle fracture at the edge. In the H900 (Figure 11) and the H1000 conditions (Figure 12), the central region is a mixture of dimpled rupture and quasi-cleavage, while the edge is almost exclusively quasi-cleavage. In the H1150 (Figure 13) and the H1150M conditions (Figure 14), the central region is composed almost completely of dimpled rupture, while the structure at the edge is observed to exhibit microplastic tearing mixed with some quasi-cleavage. When exposed to longer hydrogen charging times, specimens in the higher strength conditions exhibited instances of intergranular fracture like that observed in Figure 15 (H1000 condition, 16-hour charge).

DISCUSSION

Considerable disagreement exists in the literature concerning the influence of internal hydrogen on the mechanical properties of ferrous alloys. For example, it has long been believed that tensile strength and yield strength are not affected by hydrogen charging. Many investigators have shown that the % RA at fracture is markedly reduced. Troiano (Reference 10) found that internal hydrogen does not influence hardness, but Morris and Roopchand (Reference 12) have shown that hydrogen causes a significant increase in hardness. Most studies on the influence of strain rate on hydrogen charged metal show that HE becomes increasingly prevalent as the strain rate decreases. Tien, however (Reference 13), has proposed a mechanism indicating that susceptibility to HE is at a maximum at intermediate strain rates, becoming less important at very high or low strain rates. Taheri, et.al. (Reference 14) have shown experimentally that cathodically charged 7075 aluminum alloy in the aged condition exhibits a maximum in embrittlement at an intermediate strain rate, this strain rate increasing with degree of aging. More than likely, the above conflicts in findings are related to the mechanism by which hydrogen is transported and how it interacts in a material.

The results of this investigation show a small but consistent increase in hardness in all heat-treated conditions after hydrogen charging. This behavior implies some kind of hydrogen atom-dislocation interaction taking place, probably causing dislocation pinning to occur. This investigation also presents data indicating that at intermediate strain rates,
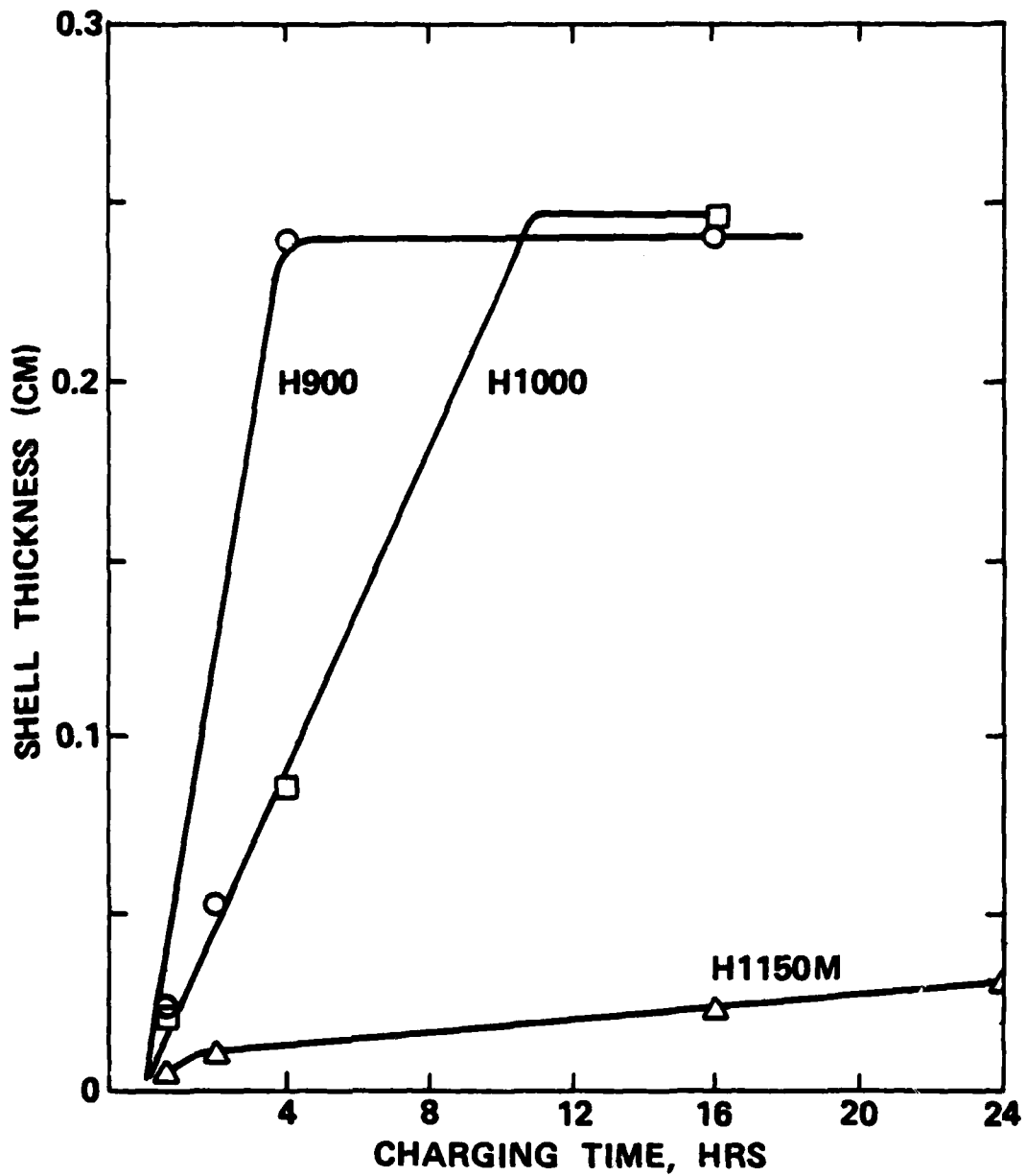
FIGURE 10. Relationship Between Shell Thickness and Hydrogen
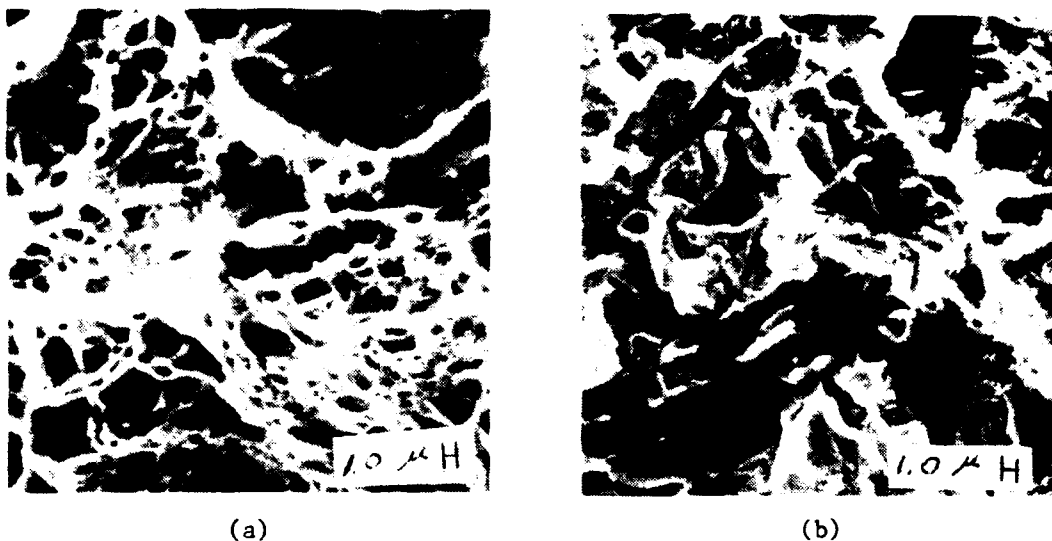Charging Time for 17-4PH in Various Aged Conditions.

FIGURE 11. SEM Fractography of 17-4PH in Condition H900
Hydrogen Charged for 2 hours, (a) Central Region Showing
Mixture at Dimpled Rupture and Quasi-Cleavage, and (b)
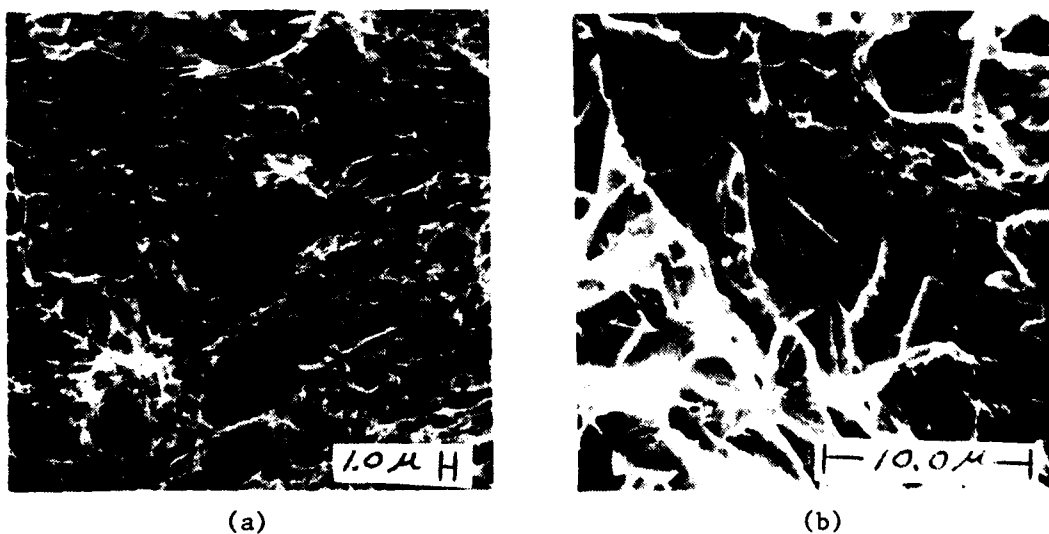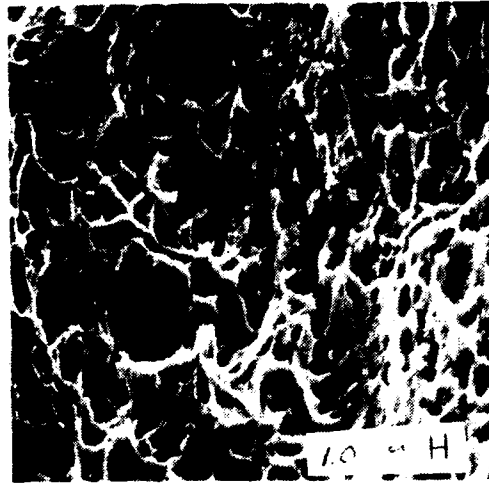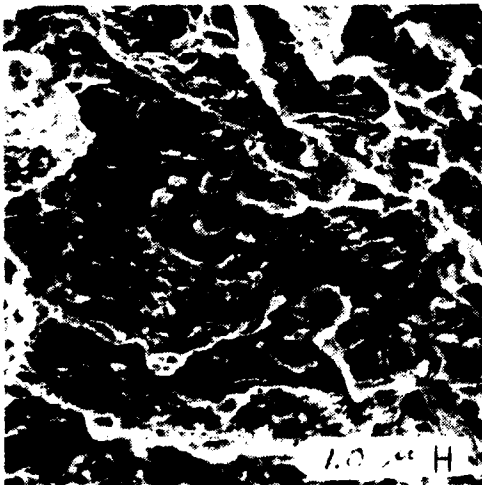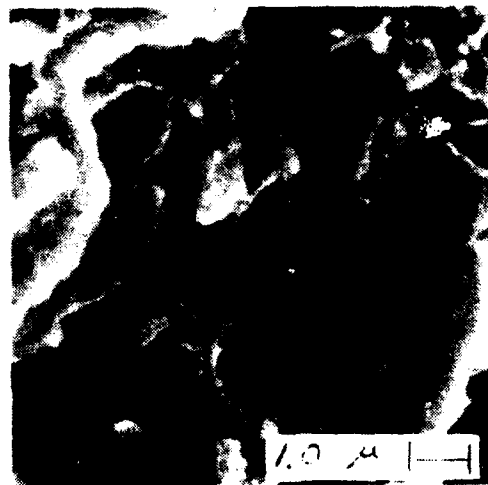Shell Region Near Edge Exhibiting Quasi-Cleavage.

FIGURE 12. SEM Fractography of 17-4PH in Condition H1000
Hydrogen Charged for 2 hours, (a) Central Region Showing
Mixture at Dimpled Rupture and Quasi-Cleavage, and (b)
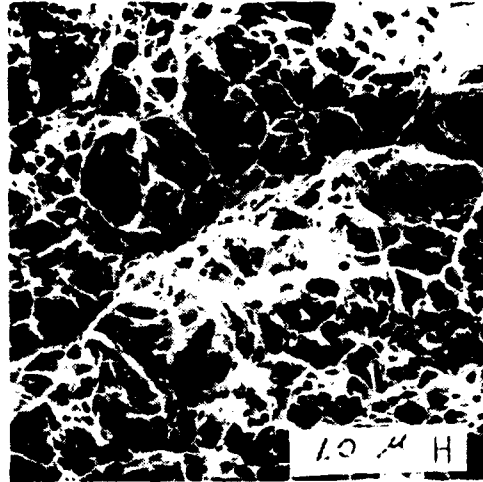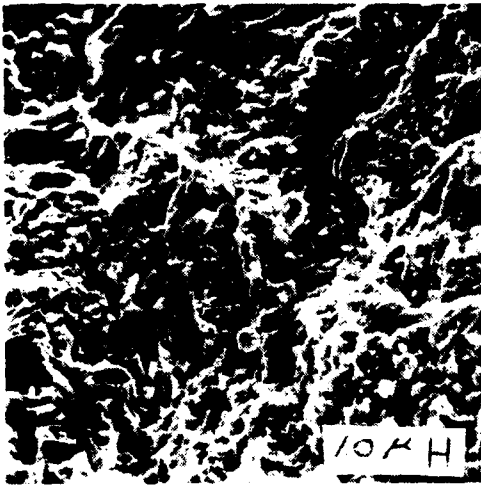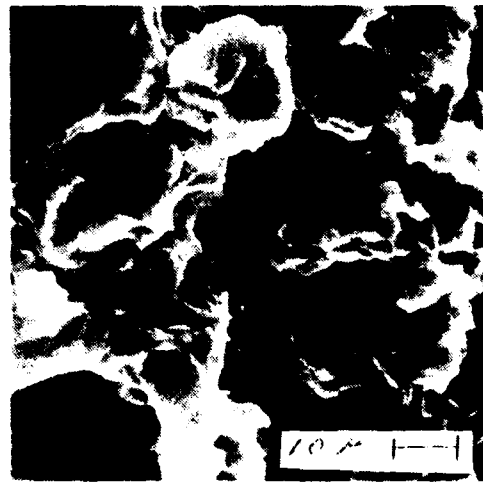Shell Region Near Edge Exhibiting Quasi-Cleavage.

(a)

(b)

(c)

FIGURE 13. SEM Fractography of 17-4PH in Condition H1150 Hydrogen Charged for 2 Hours, (a) Central Region Illustrating Dimpled Rupture, (b) and (c) Shell Region Near Edge Exhibiting Microplastic Tearing.

(a)

(b)

(c)

FIGURE 14. SEM Fractography of 17-4PH in Condition H1150M Hydrogen
Charged for 2 Hours, (a) Central Region Illustrating Dimpled Rupture,
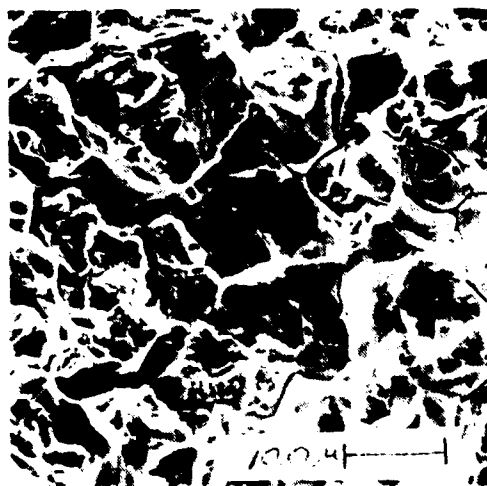(b) and (c) Shell Region Near Edge Exhibiting Microplastic Tearing.

FIGURE 15. SEM Fractography Showing Intergranular Fracture
of 17-4PH in Condition H1000 After 16 Hours Hydrogen Charge.

% RA is at a minimum. This is consistent with the mechanism proposed by Tien (Reference 13) and the experimental results of Taheri, et.al. (Reference 14). Tien discusses the existence of a critical dislocation velocity above which dislocation transport of hydrogen can no longer occur. At very low strain rates, Tien states that the rate of hydrogen enrichment is very slow. This leads to the prediction that the most severe embrittlement will occur at some intermediate strain rate, the value of which depends on hydrogen diffusivity, dislocation velocity and mobile dislocation density. For stainless steels, the critical strain rate for maximum effect of HE was estimated by Tien to be approximately 6 min^{-1}. This is in good agreement with the results found in this investigation for 17-4PH stainless steel.

The changes in fracture mode seen in this investigation are commonly observed in hydrogen embrittled alloys. The fracture mode of the specimens whose treatments yielded high strength behavior (H900, H1000 conditions) changed from primarily dimpled rupture to quasi-cleavage after hydrogen charging. The high temperature aging treatments (H1050, H1150) caused the structure to change from pure dimpled rupture to a combination of quasi-cleavage and what Thompson and Chesnutt (Reference 15) termed "tearing topography surface" (TTS).

CONCLUSIONS

1. The susceptibility of 17-4PH stainless steel to internal hydrogen embrittlement increased as cathodic charging times were increased, until saturation occurred.

2. 17-4PH stainless steel was sensitive to internal hydrogen embrittlement in all heat-treated conditions, being progressively more susceptible as strength was increased (lower aging temperature). The solution treated condition (untempered martensite) was also highly susceptible to HE.

3. Decreases in % RA and UTS, and increases in hardness were produced by hydrogen charging, the changes being recoverable on suitable outgassing.

4. The susceptibility to internal HE was shown to be a function of strain rate, the largest decrease in % RA being measured at intermediate strain rates.

5. Hydrogen charging caused the mode of fracture to change from ductile to brittle. Uncharged specimens displayed primarily dimpled rupture, while charged tensile bars exhibited quasi-cleavage and some intergranular failure.

6. The results of this investigation are consistent with dislocation-hydrogen interactions, and the ability for hydrogen to be transported through a dislocation-hydrogen transport model.

REFERENCES

1. Aerospace Corporation. *Determination of the Critical Failure Mechanism Affecting Reliability of Titan-III Bolts*, by L. Raymond and E. G. Kendall. El Segundo, Calif., June 1967. (Report No. TOR-1001 (2250-10)-2, publication UNCLASSIFIED.)

2. Naval Weapons Center. *Failure Analysis of Sidewinder Coupling Rings from the United Kingdom*, by J. L. Stokes. China Lake, Calif., NWC, December 1977. (NWC Test Report No. 3616-39-78, publication UNCLASSIFIED.)

3. A. W. Thompson. "Hydrogen-Induced Ductility Loss in Commercial Precipitation-Strengthened Stainless Steels", *Met. Trans. A.*, Vol. 7A (1976), pp. 315-318.

4. J. K. Stanley. "Stress Corrosion Cracking and Hydrogen Embrittlement of High Strength Fasteners", *J. Spacecraft*, Vol. 9, No. 11 (1972), pp. 796-804.

5. A. W. Thompson and J. A. Brooks. "Hydrogen Performance of Precipitation-Strengthened Stainless Steels Based on A-286", *Met. Trans. A.*, Vol. 6A (1975), pp. 1431-42.

6. G. T. Murray. "Hydrogen Embrittlement of 15-5PH Stainless Steels" (accepted for publication in *Met. Trans. A.*).

7. C. T. Fujii. *Stress Corrosion-New Approaches*, STP 610, ed. by H. L. Craig Jr. ASTM, Philadelphia, PA., 1976, pp. 213-225.

8. T. L. Capeletti. *Proceedings of Second International Conference on Mechanical Behavior of Materials*. ASM, Metals Park, Ohio, 1976, pp. 1489-1492.

9. I. M. Bernstein and A. W. Thompson. *Alloy and Microstructural Design*, ed. by J. K. Tien and G. S. Ansell. Academic Press, New York, 1976, pp. 303-347.

10. A. R. Troiano. *Hydrogen in Metals*, ed. by I. M. Bernstein and A. W. Thompson. ASM, Metals Park, Ohio, 1973, pp. 3-15.

11. A. W. Thompson. *Effect of Hydrogen on Behavior of Materials*, ed. by A. W. Thompson and I. M. Bernstein. AIME, Warrendale, PA., 1975, pp. 467-479.

12. J. G. Morris and B. J. Roopchand. *Environmental Degradation of Engineering Materials*, ed. by M. R. Louthan and R. P. McNitt. VPI Press, Blacksburg, VA., 1977, pp. 475-485.

13. J. K. Tien. *Effect of Hydrogen on Behavior of Materials*. AIME, Warrendale, PA., 1975, pp. 309-326.

14. M. Taheri and others. *Scripta Met.*, Vol. 13, (1979) pp. 871-875.

15. A. W. Thompson and J. C. Chesnutt. *Met. Trans. A.*, Vol. 10A (1979), pp. 1193-1196.

INITIAL DISTRIBUTION

12 Naval Air Systems Command
      AIR-00D4 (2)
      AIR-3021 (1)
      AIR-310 (1)
      AIR-320 (1)
      AIR-320A (1)
      AIR-5143 (1)
      AIR-516 (1)
      AIR-5302 (1)
      AIR-5304 (3)
 1 Naval Electronic Systems Command (Code 81341)
11 Naval Sea Systems Command
      SEA-0032 (1)
      SEA-05E (1)
      SEA-05E1 (1)
      SEA-05E3 (1)
      SEA-05ET (1)
      SEA-05EX (1)
      SEA-05M3 (1)
      SEA-62 (1)
      SEA-62C15 (1)
      SEA-99612 (2)
 2 Chief of Naval Research, Arlington
      ONR-461 (1)
      ONR-466 (1)
 1 Commander in Chief, U.S. Pacific Fleet (Code 325)
 1 Commander, Third Fleet, Pearl Harbor
 1 Commander, Seventh Fleet, San Francisco
 1 Naval Academy, Annapolis (Engineering and Weapons Division)
 1 Naval Air Engineering Center, Philadelphia (Aeronautical Materials Laboratory)
 1 Naval Air Test Center, Patuxent River (CT-252, Bldg. 405)
 1 Naval Aviation Logistics Center, Patuxent River
 3 Naval Ocean Systems Center, San Diego
      Code 131 (1)
      Code 133 (1) .
      Code P45 (1)

1 Naval Ordnance Station, Indian Head
1 Naval Postgraduate School, Monterey
1 Naval Research Laboratory (Code 510)
3 Naval Ship Weapon Systems Engineering Station, Port Hueneme
   Code 5711, Repository (2)
   Code 5712 (1)
1 Naval Surface Weapons Center, White Oak Laboratory, Silver Spring
   (Technical Library)
1 Naval War College, Newport
1 Army Armament Research and Development Command, Dover (Technical Library)
3 Army Missile Command, Redstone Scientific Information Center, Redstone Arsenal
   (DRSMI-RPRD)
2 Army Ballistic Research Laboratory, Aberdeen Proving Ground
   DRDAR-TSB-S (STINFO) (1)
1 Harry Diamond Laboratories, Adelphi (Technical Library)
1 Rock Island Arsenal
2 Watertown Arsenal
   Ordnance Materials Research Office (1)
   Technical Library (1)
1 Air University Library, Maxwell Air Force Base
3 Tactical Fighter Weapons Center, Nellis Air Force Base
   COA (1)
   CRCD (1)
   CTE (1)
2 57th Fighter Weapons Wing, Nellis Air Force Base
1 Defense Advanced Research Projects Agency, Arlington
12 Defense Technical Information Center
1 California Polytechnic State University, San Louis Obispo
   (Department of Metallurgical Engineering)
1 Carnegie-Mellon University, Pittsburgh, PA (Department of Metallurgy)
1 Case Western Reserve University, Cleveland, OH (Department of Metallurgical Engineering)
1 Colorado School of Mines, Golden, CO (Department of Metallurgy)
1 Illinois Institute of Technology, Chicago, IL (Department of Metallurgical Engineering
   and Materials Science)
1 Iowa State University of Science and Technology, Ames, IA
   (Department of Metallurgical Engineering)
1 Massachusetts Institute of Technology, Cambridge, MA (Department of Materials Science
   and Engineering)
1 Montana College of Mineral Science and Technology, Butte, MT
   (Department of Metallurgy)
1 Northwestern University, Evanston, IL (Department of Metallurgical Engineering)
1 Ohio State University, Columbus, OH (Department of Metallurgy)
1 Pennsylvania State University, State College, PA (Department of Metallurgy and
   Materials Science)
1 Purdue University, West Lafayette, IN (Department of Metallurgical Engineering)
1 Stanford University, Stanford, CA (Department of Materials Science)

26